Advances in Computer, Signals and Systems (2025)
Clausius Scientific Press, Canada

DOI: 10.23977/acss.2025.090205
ISSN 2371-8838 Vol. 9 Num. 2

High-risk area monitoring and early warning model for mountain tourism based on hyper-spectral

Bo Li[a], Xue Yan[b], Wangyu Liao[c], Xiaowei Yuan[*]

School of Information and Engineering, Sichuan Tourism University, Chengdu, 610100, China
[a]sctulibo2021@126.com, [b]13368545@qq.com, [c]liaowangyu@vip.163.com
**Corresponding author: 44016042@qq.com*

Keywords: Hyper-spectral image, Hadoop, Big data platform

Abstract: The carrier of mountain tourism is the natural environment, and the high-risk areas in the natural environment are the main hidden dangers causing safety problems, while the existing monitoring technology has the problems of low resolution, low accuracy and high false alarm rate. In this paper, a high-risk area monitoring and early warning model for mountain tourism based on hyper-spectral image(HSI) is proposed, which is called HMW, it collects Hyper-spectral images of high-risk areas through a hyper-spectral equipment and analyzes the details of high-spectral images on the Hadoop big data platform, then compose a comprehensive threshold function CEW() from multiple indicators, and trigger an alarm when the value of CEW()is greater than the risk threshold. For different types of high-risk areas, the coefficients in the CEW() function can also be adjusted, so that the CEW() function has versatility practicality. It can be seen from the simulation experiment results of the HMW model that the HMW model has the advantages of high accuracy, timely feedback and low false-positive rate, with a delay of less than 26 seconds, and can accurately and timely feedback the safety status of high-risk areas of mountain tourism.

1. Introduction

From a worldwide perspective, mountain tourism resources are extremely rich, and they are important components of tourism resources. They are key objects for the development of tourism industry various countries and an important source of tourism revenue. In the process of developing and managing mountain tourism, safety is always the primary issue and a major problem that must be solved in the development, maintenance, management and development of mountain tourism. Therefore, many researchers have proposed various safety solutions for mountain tourism from different perspectives. Generally speaking, they can be divided into two: traditional sensor technology which is used for monitoring and hight spectrum technology which is used for monitoring and analysis.

Stanciu M[1] et al. proposed a safety management model for mountain tourism, which is classified and processed according to basic data and-time sensing data; Rogowski M[2] et al. conducted real-time monitoring and evaluation based on the load index of the mountain tourist area to avoid safety problems caused excessive load; Patrichi I C[3] et al. proposed a safety strategy for

mountain tourism from the perspective of climate and environment to ensure the smooth development and management of tourism resources; Yu-Qing Z[4] et al. studied the construction of tourism risk evaluation model based on statistical and remote sensing data, fishbone diagram and entropy method according to the data of mountain tourism area; Jiang G[5] proposed a risk monitoring method, which can be used for safety monitoring of dangerous areas, but the efficiency not high; Horita[6] et al. proposed a method for disaster monitoring, but this method is only used for major disasters, which has certain limitations and selectivity. Therefore, changing the traditional way of collecting data by sensors and the technology of analyzing and processing data is an effective means to improve the accuracy and reduce the false judgment rate.

Bai Y[7] proposed a method for disaster monitoring by using high-spectral image analysis technology, and its results show the innovation and effectiveness the high-spectral in monitoring application, but the method has obvious limitations and is not suitable for high-risk area monitoring and early warning in mountain tourism; Hao J[8] achieved pollution detection by using high-spectral technology, and the high precision of high-spectral has realized the characteristic recording and identification of pollutants, which fully utilized the precision of high-spectral image technology; Belov M L[9] used high-spectral image technology to achieve the detection of the forest, and the multi-details high precision of the forest state detection were realized, and the potential danger of the forest was found in time; Huang C H[10] used high-spectral technology achieve the monitoring and analysis of air pollution, and fully utilized the high precision advantage of high-spectral technology.

From the above research results, it can be seen that the traditional sensor monitoring technology is limited by the working mode, resolution, timeliness and other factors of sensor itself, and its accuracy is generally low with a high rate of misjudgment; while the hyper-spectral technology is more used in pollution monitoring, air monitoring, and forest. However, there are few research on the monitoring of dangerous areas in mountain tourism, and there are research blind spots. Therefore, based on the above research status, this paper proposes model HMW based on the hyper-spectral technology, which is used for the monitoring and early warning of high-risk areas in mountain tourism.

2. Model and method

In order to realize the function of HMW model, it is necessary to solve the problems of real-time collection and slice preprocessing of high- areas of mountain tourism hyper-spectral images. This is the first condition to achieve monitoring. The richness and accuracy of the image directly determine the risk assessment and early warning in the followup. Second, the capacity of the high-spectrum image collected in real time is astonishing, and a single processing system is not competent. Therefore, it is necessary to use a data platform to process and analyze the high-spectrum image in a distributed and parallel way. Third, the value of the four functions of the computer, the main component change function P the detail change function D, the spectral change SC, and the structural similarity change SSIM. Using these four function values, the value of the comprehensive risk evaluation function CEW can calculated.

2.1 Acquisition and preprocessing of hyper-spectral image

Traditional sensors can only collect two-dimensional images, and have the disadvantages of low resolution, low precision, and high false alarm rate, which is not for the monitoring of high-risk areas in mountain tourism. Therefore, high-precision, multi-detail, and multi-band hyper-spectral imaging instruments are selected as data collection. The data collected by it is a hyper-spectral image, which has the advantages of high resolution, rich details, and many continuous narrow bands,

and can accurately collect object information different bands, which constitutes the data collection layer of HMW, as shown in Figure 1.

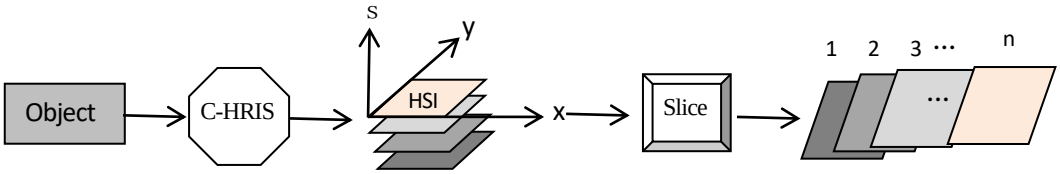

Figure 1. HSI collection and slicing

In Fig. 1, object represents the high-risk area in mountain tourism, and C-HRIS represents the hyper-spectral device. Hyperspectral image is a three-dimensional image composed of multiple two-dimensional images，x represents the width dimension, y represents the height dimension, and s represents the spectrum dimension. Since C-HRIS contains thousands of continuous narrow bands, each of which is independently imaged, so it can retain more image details which recorded the specific state of deformation, cracks, and damage in the high-order area. Slice represents the division of a hyper-spectral image into segments for analysis and processing.

2.2 Hadoop big data platform

The data collection layer slices the high-spectral image captured in real time by bands, producing a large number of two-dimensional images, which need to calculated for four components, namely, the principal component change P, the detail change D, the spectral change SC, and the structural similarity change SSIM, so as to discover whether components and details in the image have changed. If the components and details have not changed, it indicates that the high-risk area is currently not in danger, otherwise, it indicates the high-risk area is in danger of deformation, cracks, etc.

The process of computing this 4-component requires a high-performance system platform, and a single machine system is not competent due to its low performance. Therefore, Hadoop big data processing platform is chosen, which has the ability of distributed parallel processing, and the more nodes, the stronger the processing ability, as shown in Fig. 2.

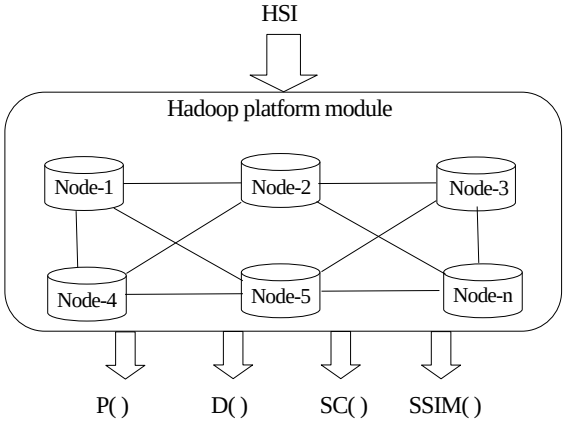

Figure 2. Structure diagram of Hadoop platform

It can be seen from Fig. 2 that when the high-spectral image HSI is input into the Hadoop platform, when the number of nodes the platform is n, the HSI is evenly divided into n parts, and each node processes 1 part. The specific process of processing is to calculate the components of the functions, and after the calculation is completed, Hadoop will splice the respective components

together, that is, the map-reduce process is completed, and the values of the 4 functions are obtained, which are P, D, SC and SSIM. These 4 functions are essential conditions for calculating the comprehensive risk evaluation function CEW subsequently.

2.3 HMW model

Based on Figure 1 and Figure 2, the calculation of comprehensive risk function CEW is added to form the HMW model, which is divided into three: data collection layer, Hadoop platform layer and evaluation and early warning layer. The three layers are combined to form the HMW model, as shown in Figure 3.

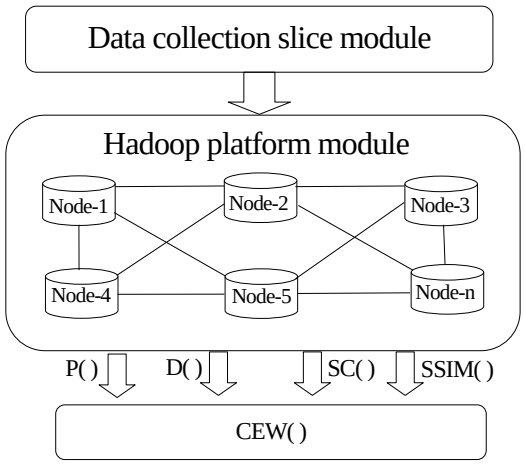

Figure 3. Structure diagram of HMW

As can be seen from Fig. 3, the HMW model contains three modules, namely: Data collection slice module, Hadoop platform module and CEW module. Three modules are executed from top to bottom to finally complete the calculation of the CEW function. Through the value of CEW, the risk state of the high-risk area of mountain tourism can be measured. When the value of CEW enters the threshold critical area, it indicates that the risk coefficient of the high-risk area is high, the alarm should be started. The computer of CEW adopts the mathematical model of form 1.

$$CEW(\mathrm{Y}) = \lambda \sum_{i=1}^{N-1} P(\mathrm{i}) + \gamma \sum_{j=1}^{M-1} D(\mathrm{j}) + \sigma \sum_{k=1}^{S} SC(\mathrm{k}) + (1 - \tau SSIM(\mathrm{x})) \tag{1}$$

In equation 1, $\lambda, \gamma, \sigma, \tau$ are the regulating coefficients, respectively, where N represents the number of main components, M represents details, S represents the number of, CEW() represents the comprehensive evaluation threshold function, P() represents the main component change function, D() represents the detail change function, SC() represents spectral change, and SS() represents the structural similarity of the image before and after the same band, and 1-ssim() then represents the degree of structural change, and when the SSIM structural changes, then the structure of the image also changes, which is an important basis for the physical change of high-risk areas.

Comparing the relationship between CEW() and threshold T, when CEW-T>= δ, δ is the critical value, it indicates that the CEW() has entered the critical area of the threshold, and the alarm is triggered, otherwise it indicates that the CEW() has not yet entered the critical area of the threshold T and is still the safe range, continue to monitor, this relationship can be expressed by equation 2.

$$W=\begin{cases}1, & \text{CEW}()-\text{T}>=\delta,\text{Alarming}\\ 0, & \text{CEW}()-\text{T}<\delta,\ \textit{Continue to monitor}\end{cases} \tag{2}$$

The workflow of HMW can be shown in a diagram, as shown in Figure 4 below.

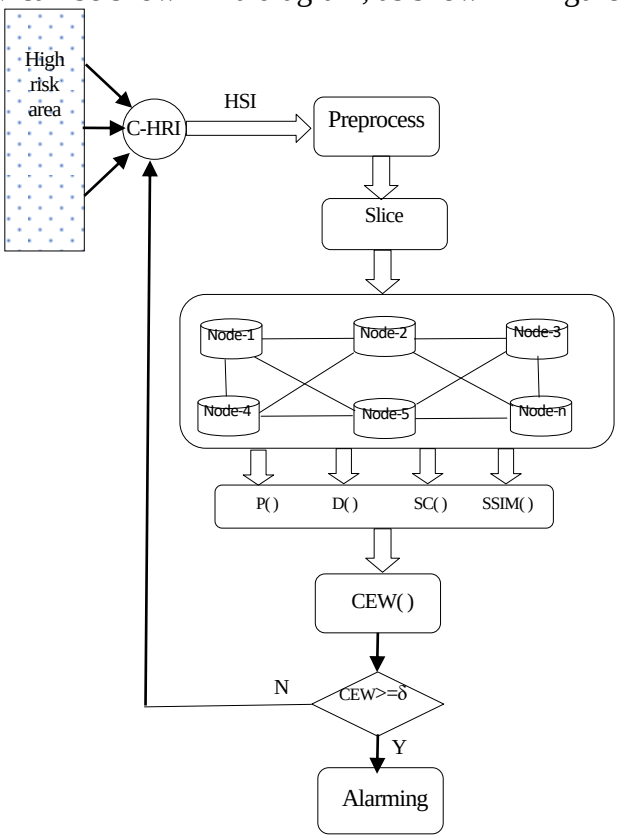

Figure 4. Workflow diagram of HMW

As can be seen from Fig. 4, the working process of the HMW model is divided into 4 steps, as described below.

Step 1, C-HRI is a hyper-spectral imager, which collects hyper-spectral images of high-risk areas, obtaining hyper-ral image HSI.

Step 2,the HSI is preprocessed, such as denoising and restoration, to obtain standardized and available HSI.

Step 3, the high-spectral image is put into Hadoop platform, and the high-spectral image is partitioned according to the number of of the platform, each node runs a piece, and when all nodes are completed, all running results are combined to obtain the values of the four functions of P(), D(), SC() and SSIM().

Step 4, the CEW() function value is calculated according to the values of the four functions P, D, SC and SSIM, and the risk threshold used to judge whether to issue an alarm.

In this process, the core goal is to obtain the values of the P, D, SC, and SSIM four functions, so as to obtain the function value CEW(), and its algorithm is shown below.

1 Initialize λ、γ、σ、τ;

2 get HSI from C-HRI;

3 Preprocessing of HSI;
4 HSI divide int pieces;
5 For i=1 to num;
6 Pi=PCA(i),Di=detail-change(i);SCi=Spectral_var(i); SSIMi=SSIM(i);
7 End for
8 P=AVG(Pi),D=AVG(Di),SC=AVG(SCi), SSIM=AVG(SSIMi);
9 CW=CEW(P,D,SC,SSIM);
10 If CW>=δ,alarming,else go 2;

3. Result Analysis and Discussion

In the simulation experiment environment, the Hadoop platform contains 50 nodes, in order to balance the completion of distributed parallel computing, the configuration of each node is the same, the hardware is DELL Precision T3660, Intel i9 12900KF, 32G memory, The capacity of the hard disk is 2T, the graphics card is NVIDIA A40000, and the network communication speed is 1000MPS. In order to simulate the multi-terminal operation, Kylinpet software is used to simulate multiple terminals.

3.1 The operation of HMW model

Hyper-spectral image is an image cube with band as the dimension, in order to quickly obtain the calculation results of HSI, HSI needs to be by band, so as to ensure that each node can obtain an HSI component. The HSI produced by the C_HRI contains 500 bands, and the current Hadoop platform has 50 nodes.So, each node can get an image of 10 bands, and each node processes the assigned image tasks in parallel. The main task of each node to calculate the value components of the P_i, D_i, SC_i and $SSIM_i$ four functions. When all nodes have completed the calculation, all the value components of the functions are. The mean value is calculated to obtain the mean value of the P, D, SC and SSIM four functions. With these mean values, the function value of CEW can calculated through Eq. 1. Here, the high-spectral image of the public data set is used as the experimental object, and the experiment is carried out with 4 randomly selected as an example to verify that the HMW model can run normally, as shown in figure. 5.

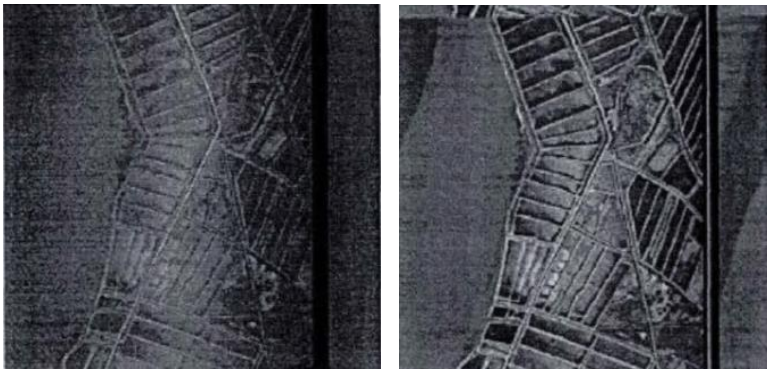

(a)Band 7 (b) band 21

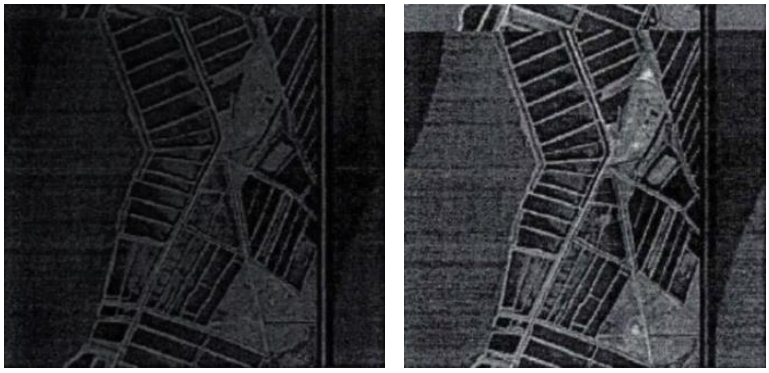

(c)Band 28 (d) band 40

Figure 5. Four bands of HSI

The values of P_i, D_i, SC_i, and $SSIM_i$ were calculated for the above four bands. Different values of the four bands will lead to different of CEW. The four adjustment coefficients were averaged with a weight of 0.25 each. When the warning threshold δ= 1.0, the results are in table 1.

Table 1. Summary of results for the same regulation coefficient

Band no	P_i	D_i	SC_i	$SSIM_i$
7	0.0162	0.1097	0.0218	0.9852
21	0.0170	0.0983	0.0301	0.9021
28	0.0205	0.0992	0.0253	0.9620
40	0.0184	0.1003	0.0231	0.9905
Avg()	0.0180	0.1019	0.0251	0.9599
CEW()	0.7563			
Alarming	FALS			

From Table 1, it can be seen that four bands of the hyperspectral image were randomly taken for calculation, and the four function value components of Pi Di, SCi and SSIMi were obtained respectively, and then according to Eq. 1, the value of CEW() could be obtained, which did not reach the threshold, so no warning was given. When $\lambda = 0.3$, $\gamma = 0.2$, $\sigma = 0.5$, $\tau = 0.1$, the bands 125, 170, 206, 25 are taken, the warning threshold δ=1, another set of function values can be obtained, as shown in Table 2.

Table 2: Summary results for different regulation coefficients

Band no	Pi	Di	SCi	SSIMi
125	0.0132	0.1120	0.0301	0.0965
170	0.0160	0.0986	0.0298	0.0921
206	0.0191	0.0921	0.0271	0.0986
255	0.0203	0.1005	0.0312	0.1004
Avg()	0.0172	0.1008	0.0296	0.2994
CEW()	0.3095			
Alarming	FALS			

From Table 1 and Table 2, it can be seen that for HSI of different bands, under the action of four adjustment coefficients, the value of CEW() can be calculated. According to the value of CEW(), the early warning decision is made. Thus it can be seen that the HMW model can operate normally.

Simulate the image change of high-risk areas in mountain tourism with the change of content in high-spectral images, and use the full variation TV of image to measure the degree of image change,

when TV is large, it indicates that the amount of image change is large；on the contrary, the amount of image change is smalland the value of CEW() function will change accordingly with the change of TV. When λ、γ、σ、τ is equal to 0.3, TV takes different values, the early warning threshold δ= 0.12, the function value and the warning situation of CEW() are shown in table 3.

Table 3. Early warning summary table

TV	Pi	Di	SCi	SSIMi	CEW	Alarming
0.01	0.0103	0.0841	0.0251	0.0816	0.09297	FALSE
0.05	0.0140	0.0915	0.0270	0.0902	0.10289	FALSE
0.10	0.0176	0.0943	0.0282	0.0942	0.10797	FALSE
0.15	0.0194	0.0986	0.0291	0.1005	0.11448	FALSE
0.20	0.0216	0.1093	0.0305	0.1210	0.13312	TRUE
0.25	0.0224	0.1207	0.0312	0.1241	0.13916	TRUE

Based on table 3, the early-warning curve of the HMW model is shown in Figure 6 when the TV value continues to increase.

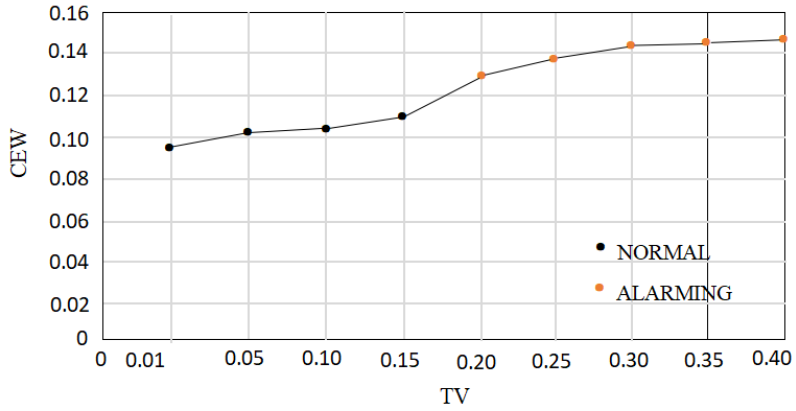

Figure 6. Early warning curve chart

In Fig. 6, TV is the total variation, which represents the amount of change in the image, and the larger the TV, the greater the CEW() value, and when the value of CEW() increases to the warning threshold δ, it indicates that the value of CEW() has reached or exceeded the risk threshold, the warning is started, and the change trend between the amount of image change and the warning is well described.

3.2 Performance experiments of the HMW model

From the above experimental data, it can be seen that in a Hadoop platform that contains 50 nodes, the high-spectral image contains 50 bands, and HMW can work normally. When the number of nodes changes, the amount of tasks for each node changes for the same HSI, and the Hadoop performance reduced. Its efficiency in calculating CEW() also changes. When $\lambda = 0.25$, $\gamma = 0.25$, $\sigma = 0.25$, $\tau = 0.1$, the efficiency of Hadoop in completing tasks is summarized in Table 4.

Table 4. Summary of HMW latency

Number of node	Band	CEW	Delay time(s)
10	1-100	0.1120	123.272
20	101-200	0.0986	71.390
30	201-300	0.0921	50.201
40	301-400	0.1005	41.689
50	401-500	0.1008	26.324

From the data in Table 4, it can be seen that with the same amount of high-spectral data, the more Hadoop nodes, the shorter latency for computing CEW. In order to demonstrate the performance change, Kylinpet was used to simulate more virtual terminals, so that the number of nodes in Hadoop continues increase, further demonstrating the law of performance change of HMW, and the results after running are summarized in Table 5.

Table 5. Summary table of HMW delay extension

Number of node	CEW	Delay time(s)
10	0.1201	140.691
40	0.0889	111.710
80	0.0940	80.239
120	0.1061	61.604
160	0.1108	35.302
200	0.1096	27.055
240	0.9803	25.971
280	0.9941	24.806
320	0.9646	24.007

Within the processing capability of the model, as the number of nodes increases, the latency will be significantly reduced, but as the number of virtual nodes increases further the latency no longer shrinks, but fluctuates around a certain latency, as shown in Figure 7.

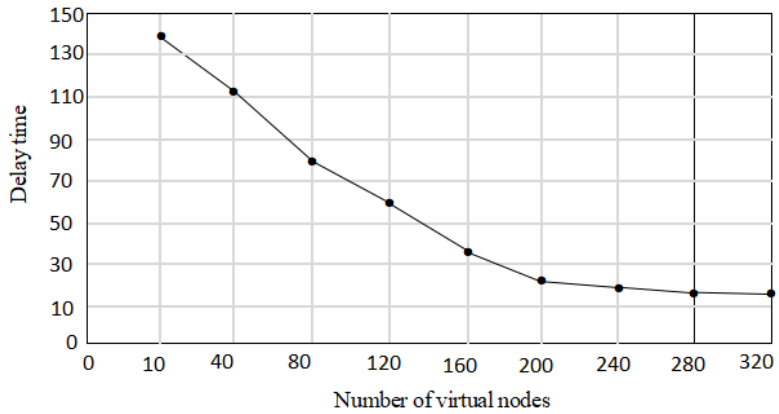

Figure 7. Delay curve diagram

As can be seen from Fig. 7, as the number of nodes increases, the ability of parallel processing is enhanced and the delay gradually decreases, but when number of nodes is too large, beyond 200, the delay tends to be stable, the parallel processing ability of the system is relatively stable, and the delay will not unrestrictedly with the increase of the number of nodes, which is consistent with the distributed parallel system.

4. Conclusion

In the paper, the HMW model integrates the high-spectral image processing technology and the big data processing technology, using the high precision and multiple details of high-spectral image to the monitoring of the high-risk area in the mountain tourism, which can obtain more details and slight deformation of the high-risk area, and can the state of the high-risk area in time, and therefore, it is the typical advantage of HMW. Moreover, in the processing of the high-spectral image, the single machine system is not used, but the Hadoop big data platform is used, and nodes in the platform can distribute and process the high-spectral image in parallel, so as to obtain the four components of the computer CEW function, and the alarm is determined to the CEW value.

From the operation and experimental results of the HMW model, it can be seen that the overall state of the HMW model is reflected in the following three aspects.

1) The HMW model can operate normally, showing good effectiveness and feasibility.

2) The efficiency of the HMW model increases with the increase in the number of nodes, and when the number of nodes reaches a certain amount, the performance of the system longer improves, but oscillates around a value.

3) The HMW model can obtain detailed details of high-risk areas, can detect subtle deformation, and can judge early warning through the CEW function, showing high accuracy.

Acknowledgement

This paper is supported by projects [2021]SCTUZK82, [2021]SCTUTP03, ZLGC2022B02 , 17ZA0286, 2025YFHZ0293 and 24SDLYAQYB024.

References

[1] Stanciu M , Popescu A , Corman S .A Model Of Good Practices In Sustainable Rural Tourism From The Mountain Area - A Case Study "Gura Raului", Sibiu County, Romania[J].Scientific Papers Series Management, Economic Engineering in Agriculture & Rural Development, 2024, 24(1).

[2] Rogowski M ,Bernadetta Zawilińska, Hibner J .Managing tourism pressure: Exploring tourist traffic patterns and seasonality in mountain national parks to alleviate overtourism effects[J].Journal of Environmental Management, 2025,373.DOI:10.1016/j.jenvman.2024. 123430.

[3] Patrichi I C. Evaluating Climate Change Adaptation Strategies For Sustaining Mountain Tourism in the Austrian Alps[J].Romanian Economic & Business Review, 2024, 19(1).

[4] Yu-Qing Z , Yue-Lin W , Hong L I ,et al.Risk assessment of mountain tourism on the Western Sichuan Plateau, China[J].Journal of Mountain Science, 2023, 20(11):3360-3375. DOI:10.1007/s11629-022-7884-6.

[5] Jiang G , Hong L J , Nelson B L .A simulation analytics approach to dynamic risk monitoring[J].IEEE Press, 2016.DOI:10.1109/WSC.2016.7822110.

[6] Horita, Flávio E.A, De Albuquerque J P , Marchezini V .Understanding the decision-making process in disaster risk monitoring and early-warning: A case study within a control room in Brazil[J].International Journal of Disaster Risk Reduction, 2018:22-31.DOI:10.1016 /j.ijdrr.2018.01.034.

[7] Bai Y , Jin X .Hyperspectral approaches for rapid and spatial plant disease monitoring[J].Trends in Plant Science, 2024(6):29.

[8] Hao J , Sun P , Li L ,et al.Application of Hyperspectral Image Recognition Technology in Monitoring the Pollution Level of Insulators[J].Applied Mathematics and Nonlinear Sciences, 2024, 9(1).DOI:10.2478/amns-2024-2988.

[9] Belov M L , Belov A M , Gorodnichev V A ,et al.Evaluation of the hyperspectral monitoring method capabilities for forests areas[J].Proceedings of SPIE, 2023, 12780(000):6.DOI:10.1117/12.2690227.

[10] Huang C H , Chen W T , Chang Y C ,et al.An Edge and Trustworthy AI UAV System With Self-Adaptivity and Hyperspectral Imaging for Air Quality Monitoring[J].IEEE Internet of Things Journal, 2024, 11(20):13. DOI:10.1109/JIOT.2024.3422470.